BIOCHEMISTRY
including biophysical chemistry & molecular biology
Article

Biochemistry **2009,** *48,* 8189–8194 8189
DOI: 10.1021/bi900958x

Association of Insulin-like Growth Factor 2 with the Insulin-Linked Polymorphic Region in Cultured Fetal Thymus Cells[†,‡]

Yuexi Wang,[§] Huiping Zhang,[§] Lee A. Ligon,[∥] and Linda B. McGown*[,§]

[§]*Department of Chemistry and Chemical Biology, Center for Biotechnology and Interdisciplinary Studies, Rensselaer Polytechnic Institute, Troy, New York 12180, and* [∥]*Department of Biology, Center for Biotechnology and Interdisciplinary Studies, Rensselaer Polytechnic Institute, Troy, New York 12180*

Received June 7, 2009; Revised Manuscript Received July 8, 2009

ABSTRACT: The insulin-linked polymorphic region (ILPR) is a regulatory sequence in the promoter region upstream of the human insulin gene and is widely recognized as a locus of type 1 diabetes susceptibility. Polymorphism of the ILPR sequence can affect expression of both insulin and the adjacent insulin-like growth factor 2 (IGF-2) gene. Several ILPR variants form G-quadruplex DNA structures in vitro that exhibit affinity binding to insulin and IGF-2. It has been suggested that the ILPR may form G-quadruplexes in vivo as well, raising the possibility that insulin and IGF-2 may bind to these structures in the ILPR in chromatin of live cells. This work establishes the presence of IGF-2 in the nucleus of cells cultured from human fetal thymus and its association with the ILPR in the chromatin of these cells. In vitro experiments support the involvement of G-quadruplex DNA in the binding interaction.

The insulin-linked polymorphic region (ILPR)[1] is a minisatellite in the promoter region of the insulin gene (INS) (*1*, *2*). It is part of the IDDM2 locus of genetic susceptibility to type 1 diabetes (also known as insulin-dependent diabetes mellitus, or IDDM), and its role in the genetics of type 1 diabetes has been the subject of numerous studies (*3*−*15*). The ILPR has been shown to influence expression of both INS and the nearby insulin-like growth factor 2 (IGF-2) genes (*16*−*18*). Allelic variations in the ILPR that are associated with high risk for type 1 diabetes are also associated with a decreased level of expression of the insulin gene in the thymus during early development (*12*, *14*, *16*, *19*−*22*). Thymic expression of pancreatic islet β cell molecules, including insulin, is critical for the development of self-tolerance; if expression is compromised, the body will produce T-lymphocytes that will attack pancreatic β cells, leading to type 1 diabetes.

The ILPR is found only in primates and is highly polymorphic in humans (*1*, *2*, *4*, *18*, *23*, *24*). Polymorphism arises both from variability in the number of tandem repeats and from variability in the frequency and distribution of the different variants of the repeat sequence that are 14−15 bases in length. It has been suggested that the ILPR may exert control over insulin and IGF-2 expression as part of a nuclear matrix attachment region that modulates accessibility of transcription factors to the corresponding genes (*16*, *17*). In this scheme, length polymorphism would tend to affect the ability of the ILPR to attach to the nuclear matrix while sequence polymorphism would tend to affect the ability of the ILPR to bind to regulatory proteins in the nuclear matrix.

Oligonucleotides containing two or more repeats of some variants, including the most prevalent "variant a" (5′-$ACAG_4TGTG_4$-3′), have been shown to form intramolecular G-quadruplex structures in vitro, and it has been suggested that G-quadruplex formation may occur in the ILPR in vivo and may be involved in its regulatory roles (*25*−*32*). For example, transcription factor Pur-1 binds to ILPR tandem repeats that form G-quadruplex structures in vitro, and insulin gene transcription rates are significantly lowered by mutations in the ILPR that destabilize the G-quadruplex structures (*32*).

Previous work has established that insulin and IGF-2 bind with high affinity in vitro to oligonucleotides comprising two-repeat sequences of ILPR variant a (ILPRa) or of ILPR variant h (ILPRh), but not of ILPR variant i (ILPRi) (*33*−*35*). The CD spectra of ILPRa and ILPRh exhibit peaks at both 260 and 295 nm, while the spectrum of ILPRi exhibits only the peak at 260 nm (*34*). While CD spectra do not unambiguously reveal specific G-quadruplex structures (*36*), these results indicate that ILPRi lacks the conformation available to ILPRa and ILPRh that results in a peak around 295 nm and is consistent with certain intramolecular G-quadruplexes such as antiparallel or propeller structures (*36*). This suggests that G-quadruplex structures of ILPRa and ILPRh are involved in their binding interactions with IGF-2 and insulin and raises the possibility that these proteins may interact with transient G-quadruplex structures in the ILPR in vivo and affect regulation of the insulin and/or IGF-2 genes.

This work focuses on establishing the presence of IGF-2 in the nuclei of cultured human fetal thymus cells (HFTCs) and determining if IGF-2 is associated with the ILPR in chromatin purified from these cells. The involvement of G-quadruplex structures in the association was investigated using an in vitro affinity capture and detection technique in which the nuclear

[†]This work was supported by National Institutes of Health Grant 1R21DK70762.
[‡]Data were deposited as GenBank accession number J00265.
*To whom correspondence should be addressed. E-mail: mcgowl@rpi.edu. Phone: (518) 276-3681. Fax: (518) 276-4887.
[1]Abbreviations: BSA, bovine serum albumin; CBS, cell blocking solution; ChIP, chromatin immunoprecipitation; HFTCs, human fetal thymus cells; HRP, horseradish peroxidase; IGF-2, insulin-like growth factor 2; IDDM, insulin-dependent diabetes mellitus; ILPR, insulin-linked polymorphic region; INS, insulin gene; IP, immunoprecipitation; NE, nuclear extract(s); PBS, phosphate-buffered saline; PBS-T, PBS containing 0.2% Tween 20; PIC, protease inhibitor cocktail; RIPA, radio-immunoprecipitation assay; T_a, ambient temperature; WCL, whole cell lysate.

Published on Web 07/09/2009

extract (NE) from the HFTCs was incubated with ILPR oligonucleotides that were covalently immobilized on fused silica probe surfaces as previously described (*37*, *38*). Captured proteins were analyzed directly on the probe surface using matrix-assisted laser desorption ionization mass spectrometry (MALDI-MS).

EXPERIMENTAL PROCEDURES

Cell Culture. A cell line derived from human fetal thymus tissue was obtained from American type Culture Collection (ATCC, Manassas, VA) (catalog no. CRL-10936). The human fetal thymus cells (HFTCs) were grown in Iscove's modified Dulbecco's medium (ATCC) with 10% fetal bovine serum (HyClone, Logan, UT), 5% human male AB serum (Fisher Scientific, Pittsburgh, PA), and 100 units/mL penicillin-streptomycin (HyClone) at 37 °C and 5% CO_2.

Whole Cell Lysate and Subcellular Fractionation. We prepared whole cell lysate (WCL) by washing confluent plates of HFTCs two times with ice-cold phosphate-buffered saline (PBS, pH 7.4) and then scraping the cells with a plastic cell scraper into 500 μL (per plate) of ice-cold radio-immunoprecipitation assay (RIPA) buffer [50 mM Tris, 150 mM NaCl, 6 mM sodium deoxycholate, 1% Triton-X 100, 0.1% SDS, and 2 mM EDTA (pH 8.0) with 5 μL of protease inhibitor cocktail III (PIC) (Research Products International Corp., Chicago, IL)]. The lysate was then transferred to a microcentrifuge tube and spun at maximum speed (17000*g*) for 5 min at 4 °C (adapted from ref *39*). Supernatants were removed and stored at −20 °C.

Nuclear extracts (NE) were prepared by differential centrifugation. All centrifuge steps were conducted at 4 °C unless otherwise stated. Confluent plates of HFTCs were first washed with 1 mL of ice-cold Dulbecco's PBS (Sigma, St. Louis, MO). An additional 1 mL of ice-cold Dulbecco's PBS was added to the plate. Cells were then scraped, transferred to a microcentrifuge tube, and spun at 850*g* for 2 min. The cell pellet was washed with 1 volume of solution A [10 mM HEPES, 1.5 mM $MgCl_2$, 10 mM KCl, 1 mM EGTA, and 1 mM EDTA (pH 7.9) with 0.1% NP-40, 1 mM dithiothreitol, and 10 μL of PIC per milliliter of solution] and centrifuged at 850*g* for 2 min. The pellet was then incubated in 1.5 volumes of solution A for 10 min on ice, followed by centrifugation at 3300*g* for 30 s. The resultant supernatant was stored at −20 °C as cytoplasmic extract. The remaining pellet was washed twice with 1 volume of solution B [20 mM HEPES, 1.5 mM $MgCl_2$, 20 mM KCl, 1 mM EGTA, and 1 mM EDTA (pH 7.9) with 0.1% NP-40, 1 mM dithiothreitol, and 10 μL of PIC per milliliter of solution] and centrifuged at 13500*g* for 10 min. The pellet was then resuspended in 0.5 volume of solution B and added dropwise while being vortexed to 0.5 volume of solution C [50 mM HEPES, 1.5 mM $MgCl_2$, 1 mM EGTA, and 1 mM EDTA (pH 7.9) with 0.1% NP-40, 1 mM dithiothreitol, and 10 μL of PIC per milliliter of solution]. The mixture was then incubated at 4 °C for 30 min and centrifuged at maximum speed for 30 min. The resultant supernatant was stored at −80 °C as NE (*40*).

Chromatin Immunoprecipitation (*ChIP*). Chromatin immunoprecipitation was performed according to the ChIP-IT Express protocol (Active Motif, Carlsbad, CA). Briefly, live HFTCs were first fixed using formaldehyde to cross-link and preserve protein−DNA interactions. The chromatin was then isolated and sheared into 100−500 bp fragments by either sonication or digestion using ChIP-IT Enzymatic Shearing Cocktail (Active Motif). Specific protein−DNA complexes were immunoprecipitated using the IGF-2 antibodies. The protein−DNA cross-linking was then reversed through incubation at 65 °C, and proteins were further removed by treatment with proteinase K. The DNA fragments of interest were recovered and analyzed using PCR.

The PCR was conducted on a MyCycler PCR machine (Bio-Rad, Hercules, CA) using the following protocol. The initial melt step was held at 94 °C for 5 min, followed by 40 cycles of 94 °C denaturing for 20 s, 50 °C annealing for 30 s, and 72 °C extension for 2 min, and then held at 4 °C. PCR primer set 1 includes 5′-ACA GGG GTG TGG GGA C-3′ as the forward primer and 5′-TTT CCA CAT TAG ACC AGG AG-3′ as the reverse primer, and primer set 2 includes 5′-ATG GCG GCA TCT TGG GCC ATC-3′ as the forward primer and 5′-TGT CCC CAC ACC CCT G-3′ as the reverse primer. All primers were procured from Integrated DNA Technologies (IDT) (San Diego, CA). PCR products were then run on a 2% agarose gel containing 1 μg/mL ethidium bromide and were imaged on a ChemiImager 4400 instrument (Alpha Innotech, San Leandro, CA).

The total DNA after fragmentation, but before precipitation, was utilized as a positive control, while the DNA bound nonspecifically to beads (with no antibody) was used as a negative control.

Western Blotting. Protein samples were first denatured in Laemmli 2× loading buffer (4% SDS, 0.1 M DTT, 20% glycerol, and 0.004% bromophenol blue in 0.125 M Tris) at a 1:1 ratio at 95 °C for 5 min. The samples were then run on a SDS−polyacrylamide gel (15%) in a running buffer [25 mM Tris, 190 mM glycine, and 0.1% SDS (pH 8.3)] at 120 V for 45 min. The proteins were transferred to an Immobilon PVDF membrane (Millipore, Billerica, MA) at 50 V for 50 min in an ice bath using a transfer buffer (25 mM Tris, 190 mM glycine, 30% methanol, and 0.005% SDS).

Membranes were then blocked in a 5% milk solution [Tris-buffered saline (pH 7.4) with 0.05% NP-40 and 5% dry milk] for 1 h at ambient temperature (T_a), rinsed with HRP buffer [100 mM Tris and 300 mM NaCl (pH 8.0) with 0.05% NP-40 and 0.1% bovine serum albumin (BSA)], and incubated with a primary antibody diluted in a mixture of a 5% milk solution/HRP buffer at a 1:1 ratio overnight at 4 °C. Membranes were then rinsed with HRP buffer and incubated with horseradish peroxidase (HRP)-conjugated secondary antibody diluted in PBS containing 0.2% Tween 20 (PBS-T) for 1 h at T_a, followed by additional rinses with PBS-T and PBS. The blots were then developed using SuperSignal West Femto substrate (Pierce Biotechnology, Rockford, IL), and chemiluminescence images were recorded on the ChemiImager 4400 instrument.

Primary antibodies used included rabbit anti human IGF-2 polyclonal antibody (AbD Serotec, Raleigh, NC), rat anti-tubulin monoclonal antibody (Chemicon, Millipore), and rabbit anti-fibrillarin polyclonal antibody (Abcam, Cambridge, MA). Secondary antibodies used included HRP-conjugated donkey anti-rabbit IgG and HRP-conjugated anti-rat IgG (Jackson ImmunoResearch, West Grove, PA). The antibody concentrations used in Western blotting were determined on the basis of manufacturers' recommendations.

Immunoprecipitation. IGF-2 antibodies (50 μL) were first immobilized onto protein A resin (150 μL of a 50% suspension) (GenScript Corp., Piscataway, NJ) through overnight incubation

at 4 °C. HFTC nuclear extracts (NE) were precleared with protein A resin (GenScript Corp.) at 4 °C for 30 min at a concentration of 150 μL of resin suspension/mL of NE to remove any nonspecific binding to the resin. The precleared NE (1 mL) was then incubated with antibody-immobilized protein A resin (200 μL) overnight at 4 °C. The beads were washed three times with ice-cold PBS buffer, suspended in 25 μL of Laemmli 2× loading buffer, and heated at 95 °C for 5 min to elute bound proteins. The eluted proteins were then analyzed using Western blotting as described above. For the control experiments, a secondary antibody rather than the primary antibody was used to precipitate proteins.

Immunocytochemistry. HFTCs were grown on glass coverslips to ~30% confluency, fixed in methanol containing 1 mM EGTA at −20 °C, rinsed with PBS, air-dried, and then blocked with cell blocking solution (CBS) (5% goat serum, 1% BSA, and 0.05% sodium azide in PBS) at 4 °C overnight. Coverslips were then incubated with a primary antibody cocktail (IGF-2 and lamin A antibodies in CBS) for 1 h at T_a or overnight at 4 °C, followed by incubation with a fluorescent secondary cocktail for 1 h at T_a. Labeled coverslips were then mounted onto slides using ProLong Gold mounting media with antifade reagent (Invitrogen, Carlsbad, CA). Cell images were recorded on a Leica inverted microscope equipped with a custom-built spinning disk confocal system (McBain Instruments, Chandler, AZ) using Volocity Software (Improvision, Waltham, MA).

Primary antibodies used included mouse anti-Lamin A monoclonal antibody (Abcam) and IGF-2 antibodies mentioned above. Fluorescent secondary antibodies included Alexa Fluor 594-conjugated anti-rabbit IgGs and Alexa Fluor 488-conjugated goat anti-mouse antibody (Molecular Probes/Invitrogen).

Affinity Protein Capture and Detection in Vitro. IGF-2 (human, recombinant, expressed in *Escherichia coli*, molecular mass of 7.5 kDa) was from Sigma. The custom-synthesized, 5′-thiol-modified oligonucleotides, including two-repeat ILPR variant a (ILPRa) [5′-$(ACAG_4TGTG_4)_2$-3′] and two-repeat ILPR variant i (ILPRi) [$(5'$-$ACAG_3TCCTG_4)_2$-3′] were from IDT. The oligonucleotides were attached to fused silica MALDI probe chips (20 mm × 20 mm × 0.75 mm) (Valley Design, Westford, MA) through a covalent linker as previously described (*33*, *34*, *37*, *38*). Immediately prior to surface attachment, oligonucleotides were heated to 95 °C for 5 min to melt any intermolecular and intramolecular structures and then cooled to room temperature in the presence of K^+ ion to promote formation of the intramolecular G-quadruplex, as confirmed by CD spectroscopy. For the affinity MALDI capture experiment, 1 μL of sample (1 μM IGF-2 standard solution or NE of HFTCs) was incubated on each oligonucleotide-modified spot at T_a for 30 min. Chips were then rinsed with deionized water for 30 s to remove any weakly bound or unbound peptides and dried under nitrogen gas. This incubation−rinse cycle was repeated two more times, each with a new 1 μL aliquot of sample, to concentrate captured proteins at the surface (*33*, *34*, *37*, *38*). MALDI matrix sinapinic acid (SA) (Sigma-Aldrich) was then applied to the spot and allowed to crystallize. The chip was then mounted on a custom aluminum MALDI target, and each spot was analyzed by MALDI-time-of-flight (TOF)-MS using a Bruker (Billerica, MA) AutoFlex II instrument. After use, the spots were rinsed with 50% acetonitrile in water to remove the MALDI matrix, proteins, and any concomitants. PBS buffer was applied to the surface to reconstitute it prior to reuse.

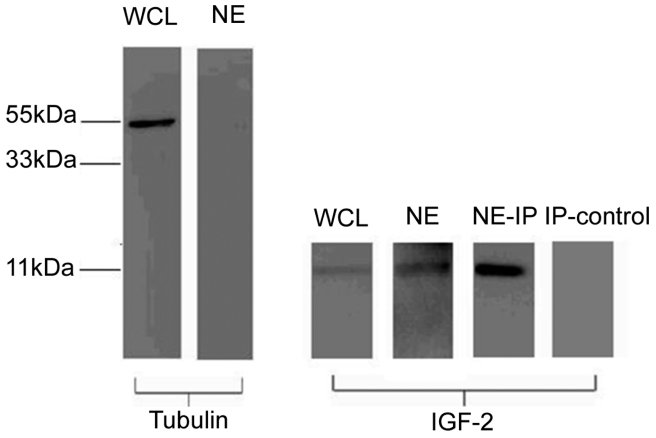

FIGURE 1: Detection by immunoprecipitation of IGF-2 in the nucleus of human fetal thymus cells. WCL, whole cell lysate; NE, nuclear extract prepared by subcellular fractionation; NE-IP, immunoprecipitation of NE with IGF-2 antibody; IP-control, NE precipitated using protein A beads. Blots were probed with an antibody to tubulin, which should be found only in the cytoplasm, to confirm efficient fractionation. Immunoprecipitated samples were probed with two or more IGF-2 antibodies to confirm results (data not shown).

RESULTS

IGF-2 Expression and Localization in HFTCs. If IGF-2 interacts with the ILPR in a physiologically relevant manner, it must enter into the nucleus. We used immunoprecipitation, immunoblotting, and immunocytochemistry to determine if IGF-2 is present in the nucleus of the cultured human fetal thymus (HFTCs). Results show that IGF-2 is strongly expressed and can be detected by immunoblotting with or without immunoprecipitation in both the whole cell lysate (WCL) and the nuclear extract (NE) (Figure 1).

To confirm the results seen by immunoblotting, we performed immunocytochemistry on cultured HFTCs (Figure 2). Three-dimensional confocal imaging was performed on HFTCs labeled with the nuclear envelope protein, Lamin A, to ensure that these puncta were indeed in the nucleus (Figure 2A). IGF-2 was typically localized to bright nuclear spots in all of the HFTCs examined [100 of 100 cells counted (Figure 2B)].

Interactions of IGF-2 with the ILPR in HFTCs. To determine if IGF-2 is associated with the ILPR region in vivo, we performed chromatin immunoprecipitation (ChIP) with antibodies to IGF-2. We probed the precipitate with PCR primer sets designed to amplify the ILPR region (Figure 3A). Therefore, if IGF-2 binds and precipitates the ILPR, we would expect to see amplification of fragments of varying lengths due to the polymorphism in this region. We observed a ladder of multiple bands with two independent primer sets from total chromatin (positive control), which indicated that our primers were appropriate (Figure 3B). We then used both primer sets to amplify DNA from the IGF-2 antibody pull-down. We observed a similar ladder of multiple bands (Figure 3B). The intensity of the products amplified by primer set 1 was lower than those amplified by primer set 2, which may represent differences in the efficiency of amplification by the two primers. Together, these data indicate that DNA containing the ILPR region is coprecipitated with IGF-2, which suggests that IGF-2 binds to the ILPR region of DNA in HFTC nuclei.

In Vitro Affinity Capture Studies. To establish a possible link between the association of IGF-2 with ILPR in

the chromatin of the live HFTCs described above and the association of IGF-2 with G-quadruplex DNA formed by the ILPRa oligonucleotide in vitro, we used an affinity MALDI-MS technique that was developed to study in vitro protein capture at oligonucleotide-modified surfaces (*37*, *38*). As described in Experimental Procedures, the sample is incubated with oligonucleotides that are immobilized at the MALDI probe surface through a covalent linker, followed by rinsing to remove unbound and weakly associated proteins and sample concomitants. Captured protein is then detected directly at the probe surface using MALDI-TOF-MS. Although formation of the intramolecular G-quadruplex by the immobilized oligonucleotides was not directly confirmed in this work, the precautions taken in the immobilization procedure to melt any preexisting structures, remove any oligonucleotides that were not covalently attached, and allow the immobilized oligonucleotides to refold in the presence of K^+ should promote the intramolecular G-quadruplex. We previously demonstrated formation of the intramolecular G-quadruplex for a thrombin-binding aptamer that was immobilized using the same procedure (*37*); verification in that case was facilitated by the prior knowledge that thrombin binds to the aptamer only when the aptamer is in its intramolecular G-quadruplex conformation.

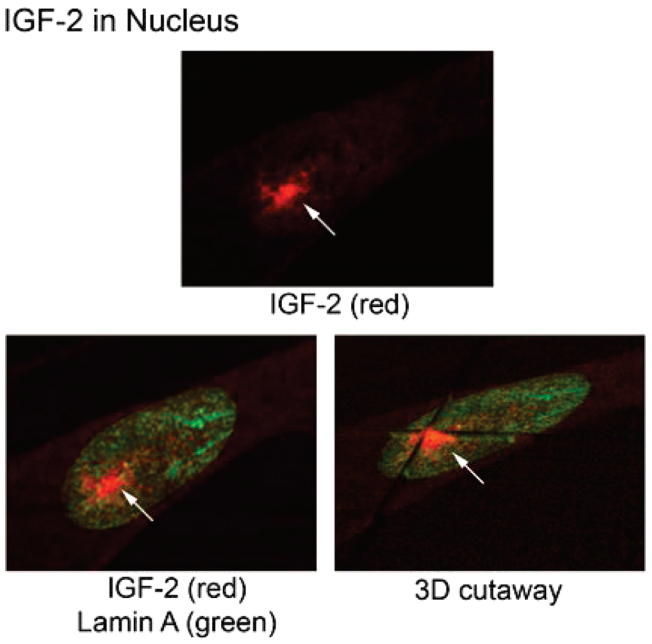

FIGURE 2: Detection of IGF-2 in HFTC nuclei in whole cells (IGF-2 found in 100 of 100 cells counted). Cells were labeled with antibodies to IGF-2 (red) and Lamin A (green, to identify the nuclear envelope). The three-dimensional image showed additional features on $X-Z$ and $Y-Z$ planes in addition to those on the $X-Y$ plane of the two-dimensional image.

Figure 4 shows affinity capture results for an IGF-2 standard solution and HFTC NE at ILPRa- and ILPRi-modified MALDI probe surfaces as well as conventional MALDI-MS spectra of the IGF-2 standard and the NE at unmodified probe surfaces. The level of capture of IGF-2 from the standard solution is much greater at the ILPRa surface (Figure 4A) than at the ILPRi surface (Figure 4B), and there is evidence of capture of IGF-2 from the HFTC NE at the ILPRa surface (Figure 4C) but not the ILPRi surface (Figure 4D). The conventional MALDI-MS spectrum of the IGF-2 standard is shown in Figure 4E for comparison with the affinity capture spectra. It yields the same IGF-2 peak as the spectrum of the protein captured from the IGF-2 standard at the ILPRa surface (Figure 4A). The conventional MALDI-MS spectrum of HFTC NE is shown in Figure 4F. It shows several small peaks, but unlike the affinity capture spectrum of HFTC NE at the ILPRa surface (Figure 4C), it does not include the IGF-2 peak. This is not surprising since there is a multitude of proteins at varying abundances and with different MALDI efficiencies in the total NE. Previous work has demonstrated the ability of the affinity MALDI-MS platform to selectively capture and concentrate specific, low-abundance proteins from complex mixtures to facilitate their detection (*37*, *38*). In this work, detection of IGF-2 in HFTC NE is achieved through affinity capture at the ILPRa-modified surface (Figure 4C) even though IGF-2 is not

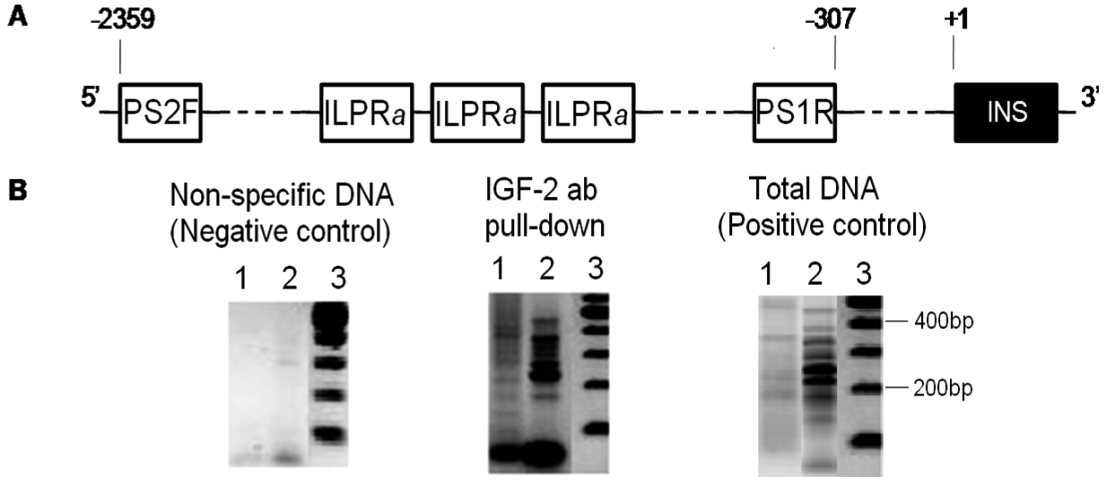

FIGURE 3: IGF-2 binding to ILPR as demonstrated by chromatin immunoprecipitation. (A) PCR primers were designed on the basis of the ILPR sequence from the INS gene (GenBank accession number J00265). For primer set 2, PS2F is the forward primer and the ILPRa sequence (ILPRa with the C-rich strand) is the reverse primer. For primer set 1, ILPRa (G-rich strand) is the forward primer and PS1R is the reverse primer. As there are many tandem repeats of ILPRa in the region from nucleotide −2359 to −307, the variant a primers should anneal to any one of these repeats, thereby resulting in a number of sequences amplified by PCR. (B) Amplified PCR products from ChIP samples and controls using primer set 1 (lane 1) and primer set 2 (lane 2). Lane 3 is standard DNA ladder. Nonspecific DNA bound to ChIP beads was used as a negative control, while total HFTC DNA was used as a positive control. Both primer sets resulted in the amplification of a ladder of multiple bands, although the intensity of those amplified by primer set 2 was higher than those amplified by primer set 1.

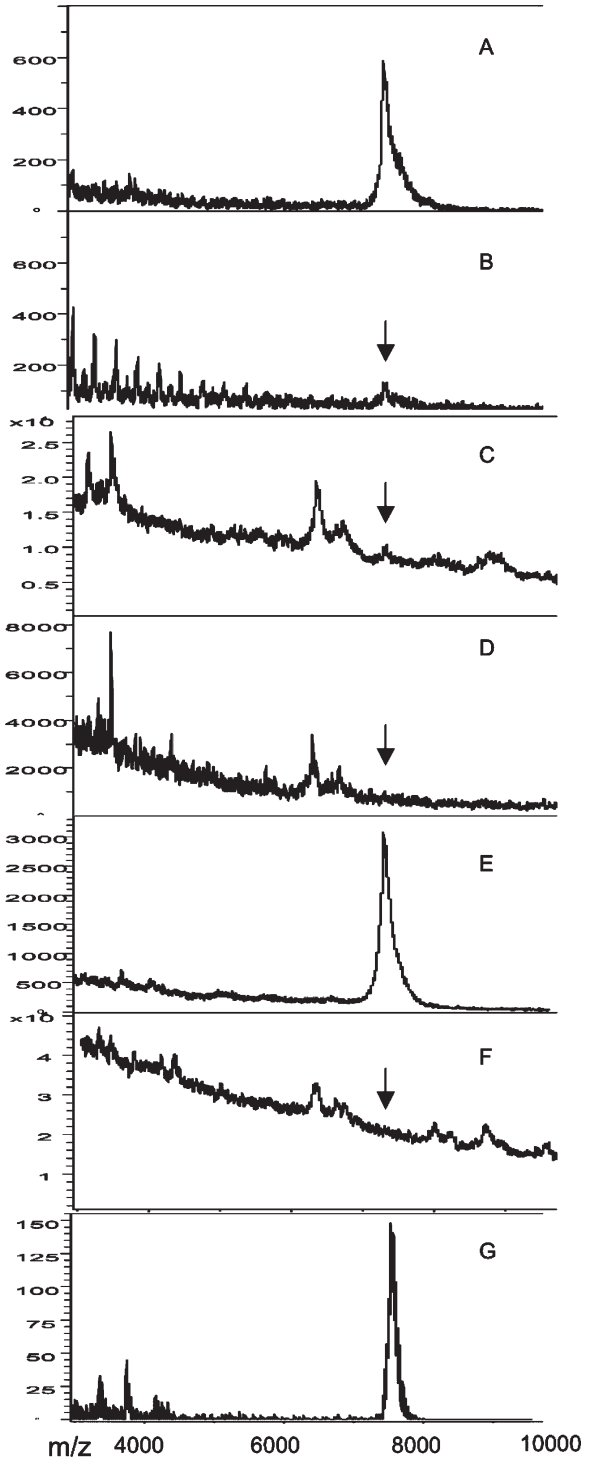

FIGURE 4: In vitro affinity MALDI-MS protein capture studies at oligonucleotide-modified MALDI probe surfaces and conventional MALDI-MS studies at unmodified MALDI probe surfaces for the IGF-2 standard and HFTC NE. (A) Capture profile of the IGF-2 standard on the ILPRa-modified surface. (B) Capture profile of the IGF-2 standard on the ILPRi-modified surface. (C) Capture profile for HFTC NE on the ILPRa-modified surface. (D) Capture profile for HFTC NE on the ILPRi-modified surface. (E) IGF-2 standard profile on the bare (unmodified) probe surface. (F) Total HFTC NE profile on the bare (unmodified) probe surface. (G) Capture profile of the HFTC NE spiked with the IGF-2 standard on the ILPRa-modified surface. Note that the relative intensity scales on the *y*-axes vary among the spectra. The arrows in some spectra indicate the *m*/*z* corresponding to the +1 ion of IGF-2 (7.5 kDa).

detected by conventional MALDI-MS of the HFTC NE (Figure 4F). Capture of IGF-2 from the HFTC NE that was spiked with IGF-2 standard on the ILPRa-modified surface (Figure 4G) confirms the ability to extract IGF-2 from the HFTC NE sample.

The results in Figure 4 confirm the presence of IGF-2 in the nucleus of HFTC and indicate that IGF-2 exhibits selective, affinity binding to ILPRa but not ILPRi. Since ILPRi lacks the CD peak exhibited by ILPRa at 295 nm that is indicative of certain intramolecular G-quadruplex structures, these results suggest that the ILPRa G-quadruplex is involved in the association with IGF-2. This is supported by previous work that showed in vitro, high-affinity capture of IGF-2 by ILPRa and ILPRh, which exhibits a CD spectrum similar to that of ILPRa, including the peak at 295 nm, but not by ILPRi (*34*).

DISCUSSION

It is becoming increasingly clear that peptides and growth factors may localize to the nucleus and directly affect transcription, in addition to their well-established effects on cell signaling in the cytoplasm (*41*−*45*). It is also clear, however, that the nuclear role of these peptides and growth factors is highly regulated and may occur only in specific tissues or circumstances (*41*, *45*). The ILPR region is thought to be an important regulatory element for the expression of both insulin and IGF-2 (*16*−*18*, *32*). The observation that IGF-2 is localized to the nucleus of HFTCs and can bind to the ILPR in HFTC chromatin is an important result with implications for insulin and perhaps IGF-2 regulation in thymus in early development. It has been suggested that insulin-mediated insulin expression may be important during early development of human thymus to allow for the establishment of immunological self-tolerance (*21*, *22*, *46*−*48*). It is worth noting that the same in vivo experiments were also performed for insulin in the HFTCs, but the results were inconclusive and are therefore not included here. In light of the in vitro studies that established affinity binding interactions between ILPR G-quadruplexes and both insulin and IGF-2 (*33*−*35*), however, further exploration of possible roles of both insulin and IGF-2 in regulating transcription of the insulin and IGF-2 genes through association with the ILPR is warranted.

A central consideration in this work is the role of G-quadruplex formation in the interactions between IGF-2 and the ILPR in the chromatin of the HFTCs. It is well established that some of the ILPR sequences form intramolecular G-quadruplex structures in vitro (*25*−*30*, *33*, *34*). Separate work has shown that ILPRa and ILPRh, either free in solution or immobilized at a surface, bind to both insulin and IGF-2 at a sequence [VCG(N)RGF] common to both proteins, where (N) is E in insulin and D in IGF-2 (*35*). It was also established that ILPRi, which does not form the G-quadruplex that gives rise to a CD peak at 295 nm, does not exhibit affinity binding to insulin or IGF-2 (*34*, *35*). It is therefore reasonable to suggest that intact IGF-2 and possibly insulin, and/or peptides derived from these proteins, may associate with the ILPR in chromatin through interactions with transient, intramolecular G-quadruplex structures similar to those formed in vitro by ILPRa and ILPRh.

ACKNOWLEDGMENT

We thank Gerri Quinones for excellent technical assistance and Matthew Rivkin for contributions to initial investigations on this subject.

REFERENCES

1. Bell, G. I., Karam, J. H., and Rutter, W. J. (1981) Polymorphic DNA region adjacent to the 5′ end of the human insulin gene. *Proc. Natl. Acad. Sci. U.S.A. 78*, 5759–5763.
2. Bell, G. I., Selby, M. J., and Rutter, W. J. (1982) The highly polymorphic region near the human insulin gene is composed of simple tandemly repeating sequences. *Nature 295*, 31–35.
3. Owerbach, D., and Nerup, J. (1982) Restriction fragment length polymorphism of the insulin gene in diabetes mellitus. *Diabetes 31*, 275–277.
4. Bell, G. I., Horita, S., and Karam, J. H. (1984) A polymorphic locus near the human insulin gene is associated with insulin dependent diabetes mellitus. *Diabetes 33*, 176–193.
5. Doria, A., Lee, J., Warram, J. H., and Krolewski, A. S. (1996) Diabetes susceptibility at IDDM2 cannot be positively mapped to the VNTR locus of the insulin gene. *Diabetologia 39*, 594–599.
6. Owerbach, D., and Gabbay, K. H. (1993) Localization of a Type I diabetes susceptibility locus to the variable tandem repeat region flanking the insulin gene. *Diabetes 42*, 1708–1714.
7. Owerbach, D., and Gabbay, K. H. (1996) The search for IDDM susceptibility genes. *Diabetes 45*, 544–550.
8. Undlien, D. E.; et al (1995) Insulin gene region encoded susceptibility to IDDM maps upstream of the insulin gene. *Diabetes 44*, 620–625.
9. Bennett, S. T.; et al (1995) Susceptibility to human type 1 diabetes at IDDM2 is determined by tandem repeat variation at the insulin gene minisatellite locus. *Nat. Genet. 9*, 284–292.
10. Ahmed, S.; et al (1999) INS VNTR allelic variation and dynamic insulin secretion in healthy adult non-diabetic Caucasian subjects. *Diabetes Med. 16*, 910–917.
11. Stead, J. D., Buard, J., Todd, J. A., and Jeffreys, A. J. (2000) Influence of allele lineage on the role of the insulin minisatellite in susceptibility to type 1 diabetes. *Hum. Mol. Genet. 9*, 2929–2935.
12. Pugliese, A. (2001) Genetic Factors in Type 1 Diabetes. In Genetics of Diabetes Mellitus (Lowe, W. L., Ed.) pp 25−42, Kluwer Academic Publishers, Dordrecht, The Netherlands.
13. Rich, S. S., and Concannon, P. (2002) Challenges and strategies for investigating the genetic complexity of common human diseases. *Diabetes 51*, S288–S294.
14. Pugliese, A., and Miceli, D. (2002) The insulin gene in diabetes. *Diabetes/Metab. Res. Rev. 18*, 13–25.
15. Maier, L. M., and Wicker, L. S. (2005) Genetic susceptibility to type 1 diabetes. *Curr. Opin. Immunol. 17*, 601–608.
16. Vafiadis, P., Grabs, R., Goodyer, C. G., Colle, E., and Polychronakos, C. (1998) A functional analysis of the role of IGF2 in IDDM2-encoded susceptibility to type 1 diabetes. *Diabetes 47*, 831–836.
17. Paquette, J., Giannoukakis, N., Polychronakos, C., Vafiadis, P., and Deal, C. (1998) The INS 5k variable number of tandem repeats is associated with IGF2 expression in humans. *J. Biol. Chem. 273*, 14158–14164.
18. Kennedy, G. C., German, M. S., and Rutter, W. J. (1995) The minisatellite in the diabetes susceptibility locus IDDM2 regulates insulin transcription. *Nat. Genet. 9*, 293–298.
19. Pugliese, A.; et al (1997) The insulin gene is transcribed in the human thymus and transcription levels correlated with allelic variation at the INS VNTR-IDDM2 susceptibility locus for type 1 diabetes. *Nat. Genet. 15*, 293–297.
20. Tait, K. F.; et al (2004) Evidence for a Type 1 diabetes-specific mechanism for the insulin gene-associated IDDM2 locus rather than a general influence on autoimmunity. *Diabetes Med. 21*, 267–270.
21. Vafiadis, P.; et al. (1997) Insulin expression in the thymus is modulated by INS VNTR alleles at the IDDM2 locus. *Nat. Genet. 15*, 289–292.
22. Chentoufi, A. A., and Polychronakos, C. (2002) Insulin expression levels in thymus modulate insulin specific autoreactive T-cell tolerance: The mechanism by which the IDDM2 locus may predispose to diabetes. *Diabetes 51*, 1383–1390.
23. Ullrich, A., Dull, T. J., Gray, A., Philips, J. A., and Peter, S. (1982) Variation in the sequence and modification state of the human insulin gene flanking regions. *Nucleic Acids Res. 10*, 2225–2240.
24. Rotwein, P., Yokoyama, S., Didier, D. K., and Chirgwin, J. M. (1986) Genetic analysis of the hypervariable region flanking the human insulin gene. *Hum. Genet. 39*, 291–299.
25. Hammond-Kosack, M. C., Dobrinski, B., Lurz, R., Docherty, K., and Kilpatrick, M. W. (1992) The human insulin gene linked polymorphic region exhibits an altered DNA structure. *Nucleic Acids Res. 20*, 231–236.
26. Hammond-Kosack, M. C., Kilpatrick, M. W., and Docherty, K. (1992) Analysis of DNA structure in the human insulin gene-linked polymorphic region *in vivo*. *J. Mol. Endocrinol. 9*, 221–225.
27. Hammond-Kosack, M. C., and Docherty, K. (1992) A consensus repeat sequence from the human insulin gene linked polymorphic region adopts multiple quadriplex DNA structures *in vitro*. *FEBS Lett. 301*, 79–82.
28. Castasti, P., Chen, X., Moyzis, R. K., Bradbury, E. M., and Gupta, G. (1996) Structure-function correlations of the insulin-linked polymorphic region. *J. Mol. Biol. 264*, 534–545.
29. Yu, Z., Schonhoft, J. D., Dhakal, S., Bajracharya, R., Hegde, R., Basu, S., and Mao, H. (2009) ILPR G-quadruplexes formed in seconds demonstrate high mechanical stabilities. *J. Am. Chem. Soc. 131*, 1876–1882.
30. Schonhoft, J. D., Bajracharya, R., Dhakal, S., Yu, Z., Mao, H., and Basu, S. (2009) Direct experimental evidence for quadruplex-quadruplex interaction within the human ILPR. *Nucleic Acids Res. 37*, 3310–3320.
31. Qin, Y., and Hurley, L. H. (2008) Structures, folding patterns, and functions of intramolecular DNA G-quadruplexes found in eukaryotic promoter regions. *Biochimie 90*, 1149–1171.
32. Lew, A., Rutter, W. J., and Kennedy, G. C. (2000) Unusual DNA structure of the diabetes susceptibility locus IDDM2 and its effect on transcription by the insulin promoter factor Pur-1/MAZ. *Proc. Natl. Acad. Sci. U.S.A. 97*, 12508–12512.
33. Connor, A. C., Frederick, K. A., Morgan, E. J., and McGown, L. B. (2006) Insulin Capture by an Insulin-linked Polymorphic Region G-Quadruplex DNA Oligonucleotide. *J. Am. Chem. Soc. 128*, 4986–4991.
34. Xiao, J., Carter, J. A., Frederick, K. A., and McGown, L. B. (2009) A genome-inspired DNA ligand for the affinity capture of insulin and insulin-like growth factor-2. *J. Sep. Sci. 32*, 1654–1664.
35. Xiao, J., and McGown, L. B. (2009) Determination of ILPR G-quadruplex binding sites in insulin and IGF-2 using MALDI-mass spectrometry. *J. Am. Soc. Mass Spectrom.* (in press).
36. Lane, A. N., Chaires, J. B., Gray, R. D., and Trent, J. O. (2008) Stability and kinetics of G-quadruplex structures. *Nucleic Acids Res. 36*, 5482–5515.
37. Dick, L. W. Jr., and McGown, L. B. (2004) Aptamer-enhanced laser desorption/ionization for affinity mass spectrometry. *Anal. Chem. 76*, 3037–3041.
38. Cole, J. R., Dick, L. W. Jr., Morgan, E. J., and McGown, L. B. (2007) Affinity capture and detection of immunoglobulin E in human serum using an aptamer-modified surface in matrix-assisted laser desorption/ionization mass spectrometry. *Anal. Chem. 79*, 273–279.
39. Hu, J, and Zhu, X (2007) Rotenone-induced neurotoxicity of THP-1 cells requires production of reactive oxygen species and activation of phosphatidylinositol 3-kinase. *Brain Res. 1153*, 12–19.
40. Dignam, J. D., Lebovitz, R. M., and Roeder, R. G. (1983) Accurate transcription initiation by RNA polymerase II in a soluble extract from isolated mammalian nuclei. *Nucleic Acids Res. 11*, 1475–1489.
41. Lin, S. Y.; et al (2001) Nuclear localization of EGF receptor and its potential new role as a transcription factor. *Nat. Cell Biol. 3*, 802–808.
42. Marti, U.; et al (2001) Nuclear localization of epidermal growth factor and epidermal growth factor receptors in human thyroid tissues. *Thyroid 11*, 137–145.
43. Reilly, J. F., and Maher, P. A. (2001) Importin β-mediated nuclear import of fibroblast growth factor receptor: Role in cell proliferation. *J. Cell Biol. 152*, 1307–1312.
44. Bryant, D. M., and Stow, J. L. (2005) Nuclear translocation of cell-surface receptors: Lessons from fibroblast growth factor. *Traffic 6*, 947–954.
45. Clevenger, C. V. (2003) Nuclear localization and function of polypeptide ligands and their receptors: A new paradigm for hormone specificity within the mammary gland?. *Breast Cancer Res. 5*, 181–187.
46. Anderson, A. C., and Kuchroo, V. K. (2003) Expression of self-antigen in the thymus: A little goes a long way. *J. Exp. Med. 198*, 1627–1629.
47. DeVoss, J.; et al (2006) Spontaneous autoimmunity prevented by thymic expression of a single self-antigen. *J. Exp. Med. 203*, 2727–2735.
48. Wicker, L. S.; et al (2005) Type I diabetes genes and pathways shared by humans and NOD mice. *J. Autoimmun. 25*, 29–33.